

TRANSFER CHARACTERISTIC OF IM₃ RELATIVE PHASE FOR A GaAs FET AMPLIFIER

Noriharu SUEMATSU, Tomonori SHIGEMATSU,
Yoshitada IYAMA and Osami ISHIDA

Information Technology R&D Center, Mitsubishi Electric Corp.
5-1-1 Ofuna, Kamakura-city, Kanagawa 247, JAPAN

ABSTRACT

Measured transfer characteristic of relative phase of the third order intermodulation distortion (IM₃) of a GaAs FET amplifier is described. The measurement system and method are also described. For drives in the weakly-nonlinear region, the measured relative phase of IM₃ is equal to that of carriers, and is well agreed with the analysis result based on Volterra-series representation. For drives in the saturation region, the measured relative phase of IM₃ versus the input power is quite larger than that of carriers relative phase. The measured results and the measurement method are useful for the design and adjustment of predistortion type linearizer for GaAs FET high power amplifiers.

I. INTRODUCTION

Both low distortion and high efficiency characteristics are desired for high power amplifiers (HPA's) used in digital radio communication systems. In order to achieve both of them, predistortion type linearizing technique has been used [1]-[5]. A predistortion type radio frequency (RF) linearizer is connected to the input port of HPA, and adds distortion components (mainly third order intermodulation distortion (IM₃)) out of phase to the carriers in phase. As the results, the distortion components, generated in the linearizer and in the HPA, are canceled out at the output port of the HPA. However, it is quite difficult to compensate the IM₃ generated in the HPA operating near saturation [4]. Since the amplitude of IM₃ generated in the linearizer can be easily adjusted to be equal to that in the HPA using a spectrum analyzer, it can be predicted that the phase of IM₃ [6] generated in the HPA has moved drastically in the saturation region.

In this paper, the relative phase of IM₃ versus the input power of a GaAs MESFET amplifier is measured. The measurement system and method are also presented.

Measured results show that (1) for drives in weakly-nonlinear region, the relative phase of IM₃ is almost equal to that of carriers, and (2) for drives near saturation, the relative phase of IM₃ moves drastically compared with that of carriers.

II. ANALYSIS BASED ON VOLTERRA-SERIES REPRESENTATION

In order to deduce the intermodulation characteristics for drives in the weakly-nonlinear region, Volterra-series analysis [7]-[8] is used. Taking into account the AM-PM conversion, the voltage transfer characteristics of an nonlinear amplifier can be obtained as follows.

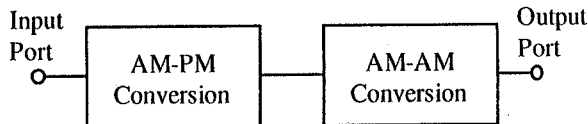


Fig.1 Model of an nonlinear amplifier.

An nonlinear amplifier can be modeled by two cascaded nonlinear elements as shown in Fig.1. One is a phase nonlinear element which represents AM-PM conversion of the nonlinear amplifier, and another is an amplitude nonlinear element which represents AM-AM conversion. For single-tone operation, the input voltage of this nonlinear amplifier v_{in} becomes

$$v_{in} = A \cos \omega_1 t \quad \dots \quad (1)$$

where A and ω_1 are the voltage amplitude and the frequency of the input signal respectively. The output voltage of the first nonlinear element (AM-PM) v_{im} can be written as

$$v_{im} = A \cos \left(\omega_1 t + \phi \left(\frac{A^2}{2} \right) \right) \quad \dots \quad (2)$$

where $\phi(A)$ represents the AM-PM conversion. Using Volterra-series representation, the output voltage of the second nonlinear element (AM-AM) v_{out} can be written as

$$\begin{aligned}
v_{out} &= \sum_{n=1}^{\infty} a_n v_{in}^n \\
&= \sum_{n=1}^{\infty} a_n A \cos^n \left(\omega_1 t + \varphi \left(\frac{A^2}{2} \right) \right)
\end{aligned} \quad \dots \dots \dots (3)$$

In the case of two-tone (ω_1, ω_2) operation, the input voltage v_{in} is

$$\begin{aligned}
v_{in} &= A \cos \omega_1 t + A \cos \omega_2 t \\
&= 2A \cos \frac{\omega_1 - \omega_2}{2} t \cdot \cos \frac{\omega_1 + \omega_2}{2} t \\
&= e(t) \cos \frac{\omega_1 + \omega_2}{2} t
\end{aligned} \quad \dots \dots \dots (4)$$

where $e(t)$ is the component of the envelope, i.e.

$$e(t) = 2A \cos \frac{\omega_1 - \omega_2}{2} t \quad \dots \dots \dots (5)$$

According to equations (1)-(5), v_{out} can be written as

$$v_{out} = \sum_{n=1}^{\infty} a_n [e(t) \cos \left(\frac{\omega_1 + \omega_2}{2} t + \varphi \left(\frac{e(t)^2}{2} \right) \right)]^n \quad \dots \dots \dots (6)$$

Here, $(v_{out})_{j=n}$ is defined as

$$(v_{out})_{j=n} = a_n [e(t) \cos \left(\frac{\omega_1 + \omega_2}{2} t + \varphi \left(\frac{e(t)^2}{2} \right) \right)]^n \quad \dots \dots \dots (7)$$

In weakly-nonlinear region, higher distortion components ($j > 3$) can be neglected, and following equations are obtained.

$$(v_{out})_{j=1} = a_1 A \left[\cos \left(\omega_1 t + \varphi \left(\frac{e(t)^2}{2} \right) \right) + \cos \left(\omega_2 t + \varphi \left(\frac{e(t)^2}{2} \right) \right) \right] \quad \dots \dots \dots (8)$$

$$\begin{aligned}
(v_{out})_{j=2} &= a_2 A^2 \left[\frac{1}{2} \cos \left(2\omega_1 t + 2\varphi \left(\frac{e(t)^2}{2} \right) \right) \right. \\
&\quad + \frac{1}{2} \cos \left(2\omega_2 t + 2\varphi \left(\frac{e(t)^2}{2} \right) \right) \\
&\quad + \cos \left((\omega_1 + \omega_2)t + 2\varphi \left(\frac{e(t)^2}{2} \right) \right) \\
&\quad \left. + \cos \left((\omega_1 - \omega_2)t + \varphi \left(\frac{e(t)^2}{2} \right) + 1 \right) \right]
\end{aligned} \quad \dots \dots \dots (9)$$

$$\begin{aligned}
(v_{out})_{j=3} &= a_3 A^3 \left[\frac{1}{4} \cos \left(3\omega_1 t + 3\varphi \left(\frac{e(t)^2}{2} \right) \right) \right. \\
&\quad + \frac{1}{4} \cos \left(3\omega_2 t + 3\varphi \left(\frac{e(t)^2}{2} \right) \right) + \frac{3}{4} \cos \left((2\omega_1 + \omega_2)t + 3\varphi \left(\frac{e(t)^2}{2} \right) \right) \\
&\quad + \frac{3}{4} \cos \left((2\omega_2 + \omega_1)t + 3\varphi \left(\frac{e(t)^2}{2} \right) \right) + \frac{9}{4} \cos \left(\omega_1 t + \varphi \left(\frac{e(t)^2}{2} \right) \right) \\
&\quad + \frac{9}{4} \cos \left(\omega_2 t + \varphi \left(\frac{e(t)^2}{2} \right) \right) + \frac{3}{4} \cos \left((2\omega_1 - \omega_2)t + \varphi \left(\frac{e(t)^2}{2} \right) \right) \\
&\quad \left. + \frac{3}{4} \cos \left((2\omega_2 - \omega_1)t + \varphi \left(\frac{e(t)^2}{2} \right) \right) \right]
\end{aligned} \quad \dots \dots \dots (10)$$

According to this set of equations(8)-(10), the relative phase of IM3 ($2\omega_1 - \omega_2, 2\omega_2 - \omega_1$) versus the input power $\frac{e(t)^2}{2}$ is equal to that of carriers (i.e. AM-PM).

III. MEASUREMENT SYSTEM AND METHOD

Figure 2 shows the configuration of the measurement system. Two carriers (2500 MHz and 2501 MHz) generated in two independent oscillators are combined, and then divided into two paths. One is connected to an amplitude transfer characteristics measurement system including device under test (D.U.T.), and another to a reference IM₃ generator. The input power of the amplifier for reference IM₃ generation is set to be constant to generate the distortion independent of the input power of the D.U.T. The output of the amplitude transfer characteristics measurement system is connected to a variable attenuator and a variable phase shifter, then combined with the output of the reference IM₃ generator, and finally connected to a spectrum analyzer.

The phase change through the path of the amplitude transfer characteristics measurement system excluding the D.U.T. is defined as φ . At the first stage, the input power is set in weakly non-linear region of the D.U.T., and the variable attenuator and the variable phase shifter are adjusted to set the spectral intensities of the two carrier components monitored by the spectrum analyzer, null. Figure 3 shows the monitored spectrum. In this case, φ is defined as φ_{C0} . Then the attenuator and the phase shifter are adjusted to set the spectral intensities of IM₃ null, as shown in Fig.4. Since there are two components of IM₃ (that is, 2499 and 2502 MHz), the phases of IM₃ are defined as φ_{L0} and φ_{H0} , respectively. Then, the same measurement procedure is continued at the next input power level, and φ_{Ci} , φ_{Li} and φ_{Hi} can be obtained. The relative phase $\Delta\varphi_{Ci}$ of carriers versus input power and the relative phase $\Delta\varphi_{Li}$ and $\Delta\varphi_{Hi}$ of IM₃ are defined as $\varphi_{Ci} - \varphi_{C0}$, $\varphi_{Li} - \varphi_{L0}$ and $\varphi_{Hi} - \varphi_{H0}$, respectively.

During this measurement, the variable attenuator and the variable phase shifter are adjusted to attain about 30dB suppression for carriers and IM₃. Figure 5 shows the relationship between signal suppression and differential power and phase of two input signals combined at the opposite phase to cancel each other. When the differential power between two signals is zero, 35.5dB and 29.0dB signal suppression, shown in Fig.3 and Fig.4, are equivalent to $\pm 1.3^\circ$ and $\pm 2.0^\circ$ measuring phase error, respectively.

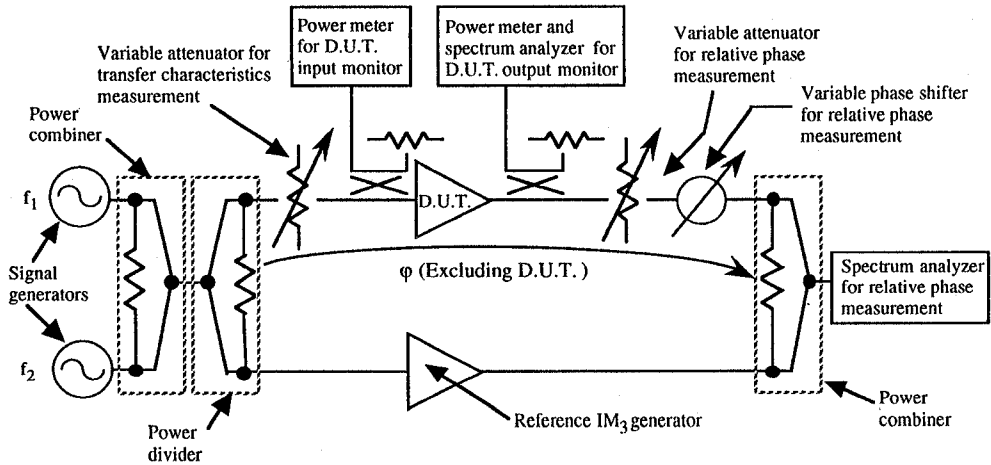


Fig.2 Configuration of the measurement system

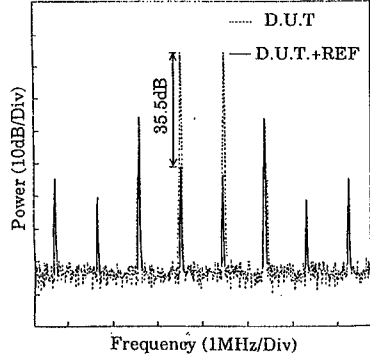


Fig.3 Spectrum under the measurement of relative phase of the carriers.

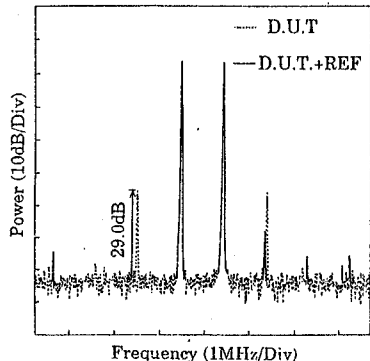


Fig.4 Spectrum under the measurement of relative phase of IM₃ (2f₁-f₂(f₂>f₁)).

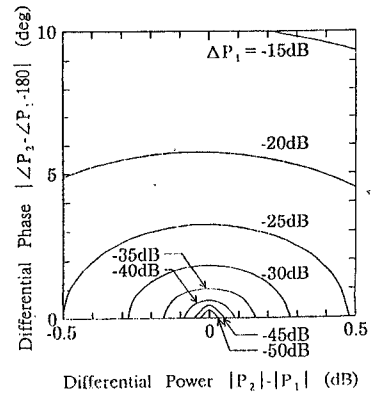


Fig.5 Relationship between signal suppression ΔP_1 and differential power and phase of two input signals (P₁ and P₂) combined at out of phase.

IV. MEASURED RESULTS

The characteristics of a 2.5GHz band class-A amplifier, using a GaAs MESFET (MGFC2407A, Mitsubishi Electric), were measured. Figure 6 shows the single-tone transfer characteristics of the amplifier. The output power at 1dB gain compression (P_{1dB}) is about 19dBm, and the relative phase of carrier is less than 5° below P_{1dB}.

Figure 7 shows the measured two-tone amplitude transfer characteristics. Below the input power of 0dBm, the amplitude of IM₃ rapidly decreases and is less than -35dBm. In this region, since the power level difference between IM₃ and noise, monitored at the spectrum analyzer, is small, enough suppression can not be achieved for the phase measurement of IM₃. As the results, the input power of the D.U.T. at the first stage of relative phase measurement is set 0dBm. Figure 8 shows the measured relative phase of carriers and IM₃ versus input power.

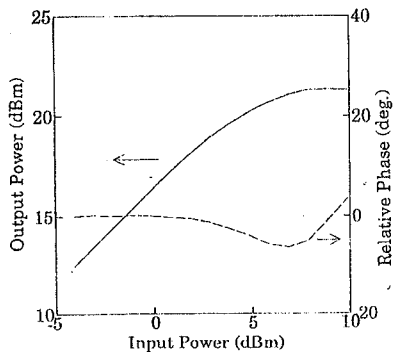


Fig.6 Single-tone transfer characteristics of GaAs MESFET amplifier.

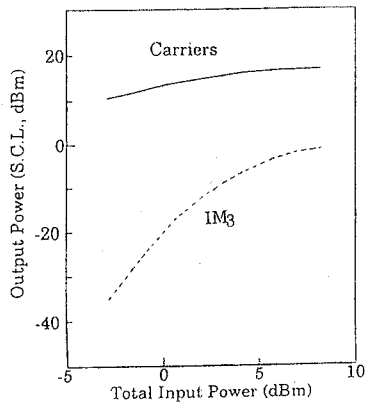


Fig.7 Input power dependence of output power of carriers and IM_3 in the case of two-tone.

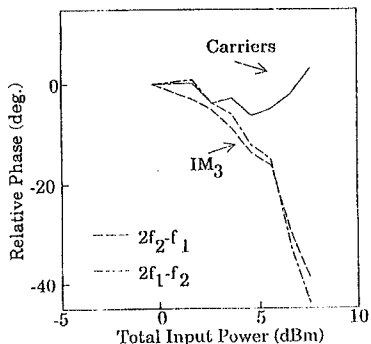


Fig.8 Input power dependence of relative phase of carriers and IM_3 in the case of two-tone.

By comparing Fig.8 with Fig.6, the magnitude of relative phase of carriers in the case of two-tone is nearly equal to that in the case of single-tone, but the locus in the case of two-tone is about 2dB shifted toward lower input power (note that the abscissa of Fig.8 is total input power). In the case of two-tone, even though the average power is equal to that in the case of single-tone, the peak power of combined waveform of two carriers is about 3dB higher

than that of single carrier. In weakly-nonlinear region, the relative phase of IM_3 is almost equal to that of carriers. For drives near saturation, the relative phase of IM_3 is quite larger than that of carriers, and the relative phase of IM_3 exceeded 30° whereas the relative phase of carriers moved below 5° .

V. CONCLUSION

Measured relative phase of IM_3 versus input power of a GaAs MESFET amplifier was described. The measurement system and method were also presented. Measured results of the GaAs MESFET amplifier demonstrated that (1) the characteristics of the relative phase of carriers versus input power in the case of two-tone had similar locus to that in the case of single-tone, (2) for drives in weakly-nonlinear region, the relative phase of IM_3 is almost equal to that of carriers as predicted in the analysis based on Volterra-series representation, and (3) for drives near saturation, the relative phase of IM_3 is quite larger than that of the carriers. Near saturation region, the relative phase of IM_3 exceeded 30° , whereas the relative phase of carriers moved below 5° .

It has been predicted that the drastically move of the relative phase of IM_3 versus the input power occurred for GaAs MESFET amplifiers operating near saturation, because of the difficulties in the adjustment of predistortion type RF linearizers. The measured results and the measurement method are useful for the design and the adjustment of these linearizers.

REFERENCES

- [1] N. IMAI, T. NOJIMA and T. MURASE, "Novel linearizer using balanced circulators and its application to multilevel digital systems", *IEEE Trans. Microwave Theory and Tech.*, vol.MTT-37(8), pp.1237-1243, Aug. 1989.
- [2] G. SATOH, "MIC linearizer for satellite communications", *Trans. Inst. Electron. Commun. Eng. Japan*, vol.J67-B no.6 pp.630-637, June 1984.
- [3] R. INADA, H. OGAWA, S. KITAZUME and P. DESANTIS, "A compact 4-GHz linearizer for space use", *IEEE Trans. Microwave Theory and Tech.*, vol.MTT-34(12), pp.1327-1332, Dec. 1986.
- [4] N. SUEMATSU, T. TAKAGI, A. IIDA, and S. URASAKI, "A predistortion type equi-path linearizer in Ku-band", *The 3rd Asia-Pacific Microwave Conference Proceedings*, pp.1077-1080, 1990.
- [5] K. YAMAUCHI, K. MORI, M. NAKAYAMA, Y. ITOH, Y. MITSUI and O. ISHIDA, "A novel series diode linearizer for mobile radio power amplifiers", *IEEE MTT-S Digest*, pp.831-834, 1996.
- [6] T. YOSHIDA, K. MONMA and K. MORITA, "Self cancellation type low distortion balanced amplifiers", *Technical report of IECE*, vol.MW76-140, pp.49-54, 1976.
- [7] R.J. WESTCOTT, "Investigation of multiple f.m./f.d.m. carriers through a satellite t.w.t. operating near to saturation", *Proc. IEE*, vol.114(6), pp.726-740, June 1967.
- [8] R.S. TUCKER, "Third-order intermodulation distortion and gain compression in GaAs FET's", *IEEE Trans. Microwave Theory and Tech.*, vol.MTT-27(5), pp.400-408, May, 1979.